Published in final edited form as:
Free Radic Res. 2013 February ; 47(2): 74–81. doi:10.3109/10715762.2012.746460.

Discriminative EPR detection of NO and HNO by encapsulated nitronyl nitroxides

Andrey A. Bobko[*], **Alexander Ivanov**, and **Valery V. Khramtsov**[*]
Division of Pulmonary, Allergy, Critical Care & Sleep Medicine, The Department of Internal Medicine, The Ohio State University, Columbus, OH 43210, USA

Abstract

Nitric oxide, •NO, is one of the most important molecules in the biochemistry of living organisms. By contrast, nitroxyl, NO^-, one-electron reduced analog of •NO which exists at physiological conditions in its protonated form, HNO, has been relatively overlooked. Recent data shows that HNO might be produced endogenously and display unique biological effects. However, there is a lack of specific and quantitative methods of detection of endogenous HNO production. Here we present a new method for discriminative •NO and HNO detection by nitronyl nitroxides (NNs) using electron paramagnetic resonance (EPR). It was found that NNs react with •NO and HNO with similar rate constants of about 10^4 $M^{-1}s^{-1}$ but yield different products: imino nitroxides and the hydroxylamine of imino nitroxides, correspondingly. An EPR approach for discriminative •NO and HNO detection using liposome-encapsulated NNs was developed. The membrane barrier of liposomes protects NNs against reduction in biological systems while is permeable to both analytes, •NO and HNO. The sensitivity of this approach for the detection of the rates of •NO/HNO generation is about 1 nM/s. The application of encapsulated NNs for real-time discriminative •NO/HNO detection might become a valuable tool in nitric oxide related studies.

Keywords

Nitric oxide; nitroxyl (HNO); nitronyl nitroxide; electron paramagnetic resonance; Angeli's salt; NONOate; liposome; nitroxide encapsulation

Introduction

It is well established that nitric oxide, •NO, can be generated in mammalian systems. On the other hand, there is no unequivocal demonstration that nitroxyl, HNO (pK_a=11.4[1, 2]), can be endogenously generated in animals. Therefore, the question of whether HNO is an endogenous signaling/effector molecule remains unanswered in spite of the demonstration of the important biological activity of HNO-releasing pharmacological agents[3-8].

Currently, there is a lack of specific and quantitative methods for detection of endogenous HNO production in biological systems[9-11]. Gas chromatography–mass spectrometry (GC-MS) detection of N_2O, the product of HNO dimerization in aqueous solutions[12], is not sufficiently sensitive due to second-order dimerization reaction, and may be nonspecific to HNO due to HNO-independent N_2O formation in living systems[13, 14]. Spectrophotometric detection of HNO reaction with transition metal complexes, such as Fe(III) metmyoglobin[15] or Mn(III) porphyrins[16], is oxygen-dependent and can hardly be

[*]Corresponding authors. Andrey A. Bobko. Andrey.Bobko@osumc.edu; tel. +1-614-292-3471; fax. +1-614-293-4799; 460 West 12th Ave., room 0360, Columbus, OH, 43210.; Valery V. Khramtsov. Valery.Khramtsov@osumc.edu; tel. +1-614-688-3664; fax. +1-614-293-4799; 473 West 12th Ave., room 201, Columbus, Ohio. .

used in biological samples. Electron paramagnetic resonance (EPR) measurement of Fe-nitrosodithiocarbamate complex with HNO[17] interferes with formation of the identical complex in the presence of •NO. HPLC detection of sulfinamide[18], product of HNO reaction with glutathione (GSH), is not specific at millimolar intracellular GSH concentrations when the main product of the reaction is oxidized glutathione. Membrane inlet mass spectrometry (MIMS) approach of HNO detection in solution can not distinguish between •NO and HNO and requires an addition of HNO-specific traps[19]. Fluorescence detection of HNO using Cu(II)-BODIPY-triazole complex suffers from nonspecific HNO-independent reduction of the complex[20]. Hydrolysis of triarylphosphine-based probes makes difficult their application for HNO detection in biological samples[21]. Therefore, the development of a sensitive, specific, quantitative and biologically compatible approach for HNO detection is essential for elucidation of physiologically-important functions of HNO.

Nitronyl nitroxides, NNs, are widely recognized as specific scavengers of nitric oxide. They have been used in numerous studies to prove •NO involvement in various physiological processes[22-27] and for •NO detection by EPR spectroscopy[22, 28-31]. The mechanism of the reaction of NNs with •NO has been well studied and the products of the reaction, imino nitroxides, INs, and $^{\bullet}NO_2$, clearly identified[22, 28-30, 32-34]. The rate constants of the reaction of the NNs with •NO were measured by stopped-flow UV-vis method[29, 33] and EPR[22] spectroscopies and was found to be equal to about 10^4 $M^{-1}s^{-1}$.

The reactivity of the NNs towards nitroxyl/HNO is much less studied. Huang et al. did not observe any EPR spectral changes at low micromolar concentrations of cPTIO nitronyl nitroxide and HNO donor, Angeli's salt (AS). However, recently Samuni[35] et al. reported conversion of cPTIO to a mixture of imino nitroxide, cPTI, and its corresponding hydroxylamine, hcPTI, at higher concentrations of AS (1 mM) and cPTIO (~200 μM). In this work we demonstrate that the product of the reaction of NNs with HNO is exclusively hydroxylamine. This allows us for the development of a new EPR approach for discriminative detection of •NO and HNO based on the formation of different products in their reactions with NNs.

Materials and Methods

Reagents

The structures of the nitronyl nitroxides, NNs, iminonitroxides, INs, and their hydroxylamines used in this work are shown in the Scheme 1.

4, 2-(4-Trimethylammoniophenyl)-4,4,5,5-tetramethylimidazoline-1-oxyl-3-oxide methyl sulfate (NN^+) and 2-(4-trimethylammoniophenyl)-4,4,5,5-tetramethylimidazoline-1-oxyl methyl sulfate (IN^+) were synthesized as previously published [29]. 2-(4-Carboxyphenyl)-4,4,5,5-tetramethylimidazoline-1-oxyl-3-oxide, monopotassium salt (cPTIO), Proli NONOate, PAPA NONOate, Angeli's salt, $Na_2N_2O_3$, were purchased from Cayman Chemicals. Sodium phosphate dibasic, Na_2HPO_4; sodium phosphate monobasic, NaH_2PO_4, were purchased from Fisher Scientific. Ascorbic acid, hydroxylamine, NH_2OH; diethylene triamine pentaacetic acid, DTPA, were bought from Acros Organics. 1,2-Dipalmitoyl-*sn*- glycero-3-phosphocholine, DPPC, was bought from Avanti Polar Lipids. Cyanamide, glutathione, catalase (1870 U/mg solid, 2310 U/mg prot.); D-(+)-glucose; glucose oxidase and palladium on carbon catalyst were purchased from Sigma-Aldrich.

Stock solutions of Angeli's salt (AS), Proli NONOate, and PAPA NONOate were prepared daily in 10 mM NaOH, concentration of AS and PAPA NONOate was determined using extinction coefficient 8300 $M^{-1}cm^{-1}$ on wavelength 248 nm[1] and extinction coefficient 8050 $M^{-1}cm^{-1}$ on wavelength 250 nm[36], correspondingly. All other solutions were

prepared in 50 mM Na-phosphate buffer (pH 7.4), 0.5 mM DTPA. Water was purified using Milli-Q purification system.

cPTI solution was prepared from corresponding solution of cPTIO by its titration with small aliquots of •NO donor, Proli NONOate, until disappearance of the EPR signal of cPTIO. The solutions of hydroxylamines of nitroxides, hcPTIO and hcPTI, were prepared by their reduction using ascorbic acid. It was found that 1 mole of ascorbic acid reduces 2.5 mole of nitroxide.

In the studies of the reaction of AS with cPTIO/hcPTIO mixture the solution of 400 μM cPTIO and 200 μM hcPTIO was prepared by addition of 80 μM of ascorbic acid to 600 μM of initial cPTIO solution. In the studies of the reactions of AS and PAPA NONOate with cPTIO/hcPTI mixture the solution of 5.7 mM cPTI was partially reduced with 2 mM of ascorbic acid yielding mixture of 5 mM hcPTI and 0.7 mM of cPTI to ensure complete oxidation of ascorbic acid. The obtained solution was used as stock for the experiments.

The solution of hIN^+ (50 mM) was prepared by reduction with hydrogen on palladium catalyst according to method [37]. The mixture containing 50 mM of hIN^+ in the presence of 5 mM of IN^+ was used as a stock solution in liposome preparation.

EPR measurements

EPR spectra were acquired in 50-μl capillary tubes using an EMX X-band spectrometer (Bruker) at room temperature.

Spectrophotometric studies

Spectrophotometric studies were performed using Varian Cary Bio and Beckman-Coulter DU800 spectrophotometers at room temperature.

Liposomes preparation

Unilamellar liposomes (100 nm diameter) from 1,2-dipalmitoyl-*sn*-glycero-3-phosphocholine, DPPC, were prepared by slightly modified extrusion method described previously[38] using LiposoFast extruder (Avestine, Inc., Ottava, Canada). A mixture of the chloroform solution of DPPC (40 mg) in 50 ml flask was dried under vacuum using rotary evaporator. The lipid film was hydrated by flask rotation in Na-phosphate buffer (50 mM, pH 7.4), DTPA (0.5 mM) containing 0.5 mM NN^+ or mixture of 0.5 mM NN^+, 0.5 mM IN^+ and 5 mM hIN^+. The resulting suspension was freeze-thawed five times in liquid nitrogen – water bath (45°C) system, and then passed through the extruder immersed in water bath (45°C). In order to remove spin label from the outer liposomal volume, the liposome suspension was passed through a gel-filtration column (Sepharose CL2B, 15 × 0.8 cm) equilibrated with the same buffer, and the liposome fraction was collected afterwards. Encapsulating efficiency, 4.4±0.3 %, was determined from comparison of EPR spectra intensity of final liposome preparation with initial solution.

Results and Discussion

EPR observation of the reaction of nitronyl nitroxides with •NO and HNO

As has been shown in numerous previous studies, NNs react with •NO resulting in stoichiometric formation of INs[22, 28-30, 32-34]. Figure 1A and 1B show the structures of the cPTIO and cPTI and their EPR spectra characterized by quintet and septet pattern, correspondingly.

The reactivity of the NNs towards nitroxyl/HNO is less studied. To study this reaction we used commonly used HNO donor, AS. Similar to the reaction of NNs with $^{\bullet}$NO, we observed transformation of the EPR spectrum of cPTIO to cPTI upon cPTIO incubation with AS. The corresponding EPR-measured kinetics of cPTIO decay and cPTI accumulation are shown in Fig. 1C (circles). However, the characteristic time of the kinetics, $\tau_{1/2}\approx$1.5 min, was about 10-fold lower than half lifetime of spontaneous AS decomposition (16-18 min at 25 °C[39, 40]). Recently Samuni[35] et al. reported conversion of cPTIO to a mixture of cPTI and its hydroxylamine, hcPTI (see Scheme 1 for the structures), upon incubation in the presence of AS. In agreement with our data the authors reported several fold faster rates of the cPTIO conversion compared with the rate of spontaneous AS decomposition but did not discuss the observed discrepancy in the paper. We hypothesized here that the fast transformation of the EPR spectra of NNs in the presence of AS might be a consequence of NN-facilitated oxidative AS decomposition, the mechanism of which will be discussed below. Note that previously an oxidative mechanism of accelerated AS decomposition via $^{\bullet}NO_2$-initiated free radical chain reaction was proposed to explain AS instability in acidic medium[39]. To test the hypothesis we used hydroxylamine of cPTI as a mild reducing agent and radical scavenger to prevent possible oxidative decomposition of AS. An addition of hcPTI (Fig. 1C, squares) slowed down EPR-measured cPTIO decay which proceeded with $\tau_{1/2}$ about 14 min being close to half lifetime of AS decomposition. cPTI radical formed in these conditions might be either a product of cPTIO reaction with HNO or product of hcPTI oxidation. To discriminate between these possibilities, we used alternative reducing agent, hcPTIO (Scheme 1), instead of hcPTI. Interestingly, we did not observe any EPR spectral transformations in the presence of hcPTIO, therefore not supporting cPTI formation in the reaction of HNO with cPTIO. Nevertheless, the spectrophotometric studies of HNO reaction with cPTIO in the presence of hcPTIO revealed transformation of EPR-silent diamagnetic species, namely stoichiometric conversion of hcPTIO to hcPTI with the same characteristic time, $\tau_{1/2}\approx$14 min (see next Section) as in case of EPR-measured reaction (cf. Figs. 1C and 2C). We found the only mechanism of HNO reaction with NNs which is consistent with the both observations, namely:

$$\mathrm{NN}+\mathrm{HNO} \rightarrow \mathrm{hIN}+{}^{\bullet}\mathrm{NO}_2 \quad (1)$$

In case of mixture of cPTIO and hcPTI the reaction (1) with HNO results in:

$$\mathrm{cPTIO}+\mathrm{HNO} \rightarrow \mathrm{hcPTI}+{}^{\bullet}\mathrm{NO}_2 \quad (1a)$$

$$\mathrm{hcPTI}+{}^{\bullet}\mathrm{NO}_2 \rightarrow \mathrm{cPTI}+\mathrm{HNO}_2 \quad (2)$$

with the net equation

$$\mathrm{cPTIO}+\mathrm{HNO} \rightarrow \mathrm{cPTI}+\mathrm{HNO}_2 \quad (3)$$

being consistent with EPR-observed stoichiometric conversion of cPTIO to cPTI.

In case of mixture of cPTIO and hcPTIO the reaction (1) results in the different final products, namely:

$$\mathrm{cPTIO}+\mathrm{HNO} \rightarrow \mathrm{hcPTI}+{}^{\bullet}\mathrm{NO}_2 \quad (1a)$$

$$\mathrm{hcPTIO}+{}^{\bullet}\mathrm{NO}_2 \rightarrow \mathrm{cPTIO}+\mathrm{HNO}_2 \quad (4)$$

with the net equation

$$\mathrm{hcPTIO + HNO \rightarrow hcPTI + HNO_2} \quad (5)$$

being consistent with the absence of EPR spectra changes and presence of optically-observed stoichiometric conversion of hcPTIO to hcPTI (see next Section).

Note, that $^{\bullet}NO_2$–induced conversion of hydroxylamines, hcPTIO and hcPTI, to the corresponding nitroxides, cPTIO and cPTI, may proceed via two-step mechanism. First, $^{\bullet}NO_2$ oxidizes cPTIO to the oxoammonium cation, which, in turn, oxidizes hcPTIO or hcPTI. The rate constant of $^{\bullet}NO_2$-induced oxidation of hcPTIO ($\leq 10^5$ $M^{-1}s^{-1}$)[41, 42] is more than two orders of magnitude lower than that for oxidation of cPTIO (1.5×10^7 $M^{-1}s^{-1}$) [33] supporting two-step mechanism.

Spectrophotometrical studies of the reaction of nitronyl nitroxides with HNO

The optical spectra of cPTIO, hcPTIO, cPTI, and hcPTI compounds are shown in Fig. 2A.

Fig. 2B shows the differential optical spectra of the mixture of cPTIO and hcPTIO measured at different time intervals after addition of AS. The spectra pattern transformation is characterized by isosbestic point at 340 nm which indicates conversion of hcPTIO to the hcPTI (Fig. 2A) upon HNO release by AS. Fig. 2C shows the kinetics of hcPTIO conversion to hcPTI monitored at 299 nm with stoichiometry hcPTIO:hcPTI=1:1 and $\tau_{1/2}$=(14±1) min which are in a good agreement with EPR data (Fig. 1C) and previously published $\tau_{1/2}$ ~16 min for AS decomposition at 25 °C[39, 40].

The EPR spectrum of the reaction mixture of cPTIO and hcPTIO consisted of the cPTIO signal only and was not changed during the reaction (data not shown). The observed data are in agreement with the predicted net reaction (5).

The proof of the reaction mechanism of NN with HNO

Our experiments show that the use of AS as a source of HNO requires special precautions to prevent NN-induced oxidative decomposition of AS. Therefore, the corresponding EPR and optical studies were performed in the presence of mild reducing agents, hcPTIO or hcPTI. The decay of the EPR signal of the NN (Fig. 1C) proves reactivity of the NN with HNO which was assigned to the formation of EPR-silent product, hIN, according to reaction (1). The appearance of EPR signal of the IN was explained by oxidation of corresponding hIN according to reaction (2). It is desirable to confirm HNO-induced transformation of the NN to a diamagnetic IN product in a simple reaction mixture when direct interaction between the source of HNO generation and detecting probe is excluded.

Previously we have shown that positively charged NN^+ does not penetrate phospholipid membranes and can be encapsulated in inner aqueous volume of liposomes[29]. Here we used liposome-encapsulated NN^+ to exclude direct interaction between NN^+ and HNO donor. An enzyme-catalyzed oxidation of cyanamide by hydrogen peroxide in the presence of catalase[43] has been used as membrane-impermeable source of HNO. Note that small neutral HNO molecule freely diffuses across phospholipid barrier of the liposomes. The observed decay of the EPR signal of liposome-encapsulated NN^+ and absence of any other EPR signal appearance in the presence of HNO generating enzymatic system (Fig. 3) unambiguously confirm the conversion of the NN into diamagnetic product in agreement with the reaction (1). As seen in Figure 3 this conversion was completely abolished by addition of HNO scavenger, glutathione ($k_{sc}\approx10^6$ $M^{-1}s^{-1}$ [7]).

Measurement of bimolecular rate constant of nitronyl nitroxide reaction with HNO

The rate constant of the reaction of cPTIO with HNO, k_{1a}, was measured using NH_2OH as competitive reagent. NH_2OH reacts with HNO yielding N_2 and H_2O[40] with the rate constant, k_H =0.4×10^4 M^{-1}s^{-1} [44]. Fig. 4A shows the initial rates of hcPTIO conversion to hcPTI measured at wavelength 299 nm after addition of AS to solutions containing hcPTIO/cPTIO mixture in the absence (V_0) and presence (V) of various concentrations of NH_2OH. Fig. 4B shows linear dependence of the term ($V/V_{0\text{-}1}$) on NH_2OH concentration with the slope yielding the bimolecular rate constant, k_{1a} = (5.5±0.9)×k_H = 2.2×10^4 M^{-1} s^{-1}. The obtained value of the rate constant of HNO reaction with cPTIO is an order of magnitude lower than that reported by Samuni et al.[35]. The authors did not take into account cPTIO-induced acceleration of AS decomposition, which resulted in overestimation of the rate constant of the reaction of cPTIO with HNO.

EPR detection of •NO and HNO by nitronyl nitroxide/hydroxylamine detecting system

The capacity of EPR detection of •NO and HNO by NN in the presence of hIN was explored for two NNs, cPTIO and NN$^+$ (see Scheme 1) using PAPA NONOate and AS as sources of •NO and HNO, correspondingly. Figure 5 shows the rates of the EPR-measured NN decay and IN accumulation in the presence of PAPA NONOate and AS. The rates of NN decay linearly depended on the concentrations of PAPA NONOate and AS yielding half lifetimes of their decomposition, $\tau_{1/2}$ = (88±2) min and $\tau_{1/2}$ = (14.0±0.2) min, correspondingly, in a good agreement with the literature data. However, the stoichiometry of the transformation, Δ[NN]/Δ[IN], was found to be significantly different, being close to 1:2 in case of •NO generation and 1:1 in case of HNO generation. This is in agreement with the different mechanisms of •NO and HNO reactions with the NNs. In case of •NO generation, the observed transformations are described by equations:

$$\mathrm{NN} + {}^{\bullet}\mathrm{NO} \rightarrow \mathrm{IN} + {}^{\bullet}\mathrm{NO_2} \quad (6)$$

$$\mathrm{hIN} + {}^{\bullet}\mathrm{NO_2} \rightarrow \mathrm{IN} + \mathrm{HNO_2} \quad (7)$$

with the net equation

$$\mathrm{NN} + \mathrm{hIN} + {}^{\bullet}\mathrm{NO} \rightarrow 2 \times \mathrm{IN} + \mathrm{HNO_2} \quad (8)$$

being consistent with EPR-observed stoichiometry Δ[NN]/Δ[IN] close to 1:2 (Fig. 5A).

In case of HNO generation, the observed transformations are described by equations (1-3) being consistent with EPR-observed stoichiometry Δ[NN]/Δ[IN] close to 1:1 (Fig. 5B). The observed •NO- and HNO-induced EPR spectral changes of NNs in the presence of hIN can be used as calibration for further quantitative EPR measurements of the rates of •NO/HNO generation. The different stoichiometry of the Δ[NN]/Δ[IN] transformation can be used for discriminative •NO and HNO detection as demonstrated in the next section.

Discriminative detection of nitric oxide and HNO by encapsulated nitronyl nitroxides

The application of NNs in biological systems is limited due to the fast reduction of NNs and INs into diamagnetic EPR-silent product[29, 32, 45]. Encapsulation of membrane-impermeable NNs into the inner aqueous space of the liposomes has been previously used to protect NNs against bioreduction[29, 30, 46, 47]. Here we explore the utility of encapsulated NN$^+$ for discriminative detection of •NO and HNO. Both species, HNO and •NO, freely diffuse across phospholipid membrane, then react with the NN$^+$ forming different products, paramagnetic IN$^+$ and diamagnetic hIN$^+$, correspondingly. The latter should result in the different spectra changes as shown in Figure 6 illustrating the concept of this EPR approach.

To demonstrate the capacity of encapsulated membrane-impermeable NN^+ probe for discriminative detection of $^{\bullet}NO$ and HNO we performed EPR measurements using PAPA NONOate as $^{\bullet}NO$ donor and AS as HNO donor. An addition of AS to the liposome-encapsulated NN^+ resulted in several-fold acceleration of AS decomposition probably due to penetration of $^{\bullet}NO_2$ and/or AS across the lipid bilayer. Therefore in the following experiments we used the liposome-encapsulated equimolar mixture of NN^+ and IN^+ in the presence of excess of hIN^+ as $^{\bullet}NO$/HNO detecting system. The use of equimolar concentrations of NN^+ and IN^+ enhanced an accuracy of detection of small changes of their EPR spectra while excess of hIN^+ ensured complete scavenging of oxidizing species, $^{\bullet}NO_2$ and oxoammonium cations. Figure 7A shows the EPR-measured decays of the NN^+ radical in the presence of PAPA NONOate, AS and both of them. The rates of the observed NN^+ decays were in a good agreement with the corresponding calculated rates of generation of nitric oxide by PAPA NONOate, HNO by AS or both of these species (see Table 1). In all three cases the NN^+ signal decay was accompanied by the increase of IN^+ signal (Fig. 7B). The stoichiometry of the transformation, $\Delta[NN^+]/\Delta[IN^+]$, was found to be significantly different being close to 1:2 in case of $^{\bullet}NO$ generation and 1:1 in case of HNO generation (Fig. 7C and Table 1). This is in agreement with the different reaction mechanisms of $^{\bullet}NO$ (eqs. 6-8) and HNO (eqs.1-3) with the components of detecting system (see previous section).

In case of simultaneous •NO and HNO generation we observed the intermediate value of stoichiometry, $\Delta[NN^+]/\Delta[IN^+]=1.25$, being close to the value calculated from the rates of $^{\bullet}NO$ and HNO generation and the values 1:2 and 1:1 for the stoichiometries of the net reactions (8) and (3) (see Table 1).

Therefore, an addition of hIN to NN (i) eliminates possible harmful effects of $^{\bullet}NO_2$ on the studied system by its scavenging and (ii) provides possibility of discriminative detection of $^{\bullet}NO$ and HNO based on different stoichiometry of NN conversion to IN.

Conclusion

It has been shown that NNs react with $^{\bullet}NO$ and HNO with the comparable rate constants of about 10^4 $M^{-1}s^{-1}$ but form different products (IN and hIN, respectively), as well as highly reactive $^{\bullet}NO_2$ radical. An addition of the hydroxylamine, hIN, to NN provides scavenging of harmful $^{\bullet}NO_2$ radical eliminating its possible toxic effect in biological system. The mixture of NNs and hINs represents an useful EPR detecting system which allows for discriminative quantitative EPR detection of $^{\bullet}NO$ and HNO based on different stoichiometry of NN conversion to IN. The sensitivity of this approach for the detection of the rates of $^{\bullet}NO$ or/and HNO generation is about 1 nM/s. Encapsulation of the mixture of charged NN^+ and hIN^+ into the liposomes allows for this approach to be applicable in the reducing environments of biological systems.

Acknowledgments

This work was partly supported by NIH grant HL089036.

REFERENCES

[1]. Shafirovich V, Lymar SV. Nitroxyl and its anion in aqueous solutions: spin states, protic equilibria, and reactivities toward oxygen and nitric oxide. Proc Natl Acad Sci U S A. 2002; 99:7340–7345. [PubMed: 12032284]

[2]. Bartberger MD, Liu W, Ford E, Miranda KM, Switzer C, Fukuto JM, Farmer PJ, Wink DA, Houk KN. The reduction potential of nitric oxide (NO) and its importance to NO biochemistry. Proc Natl Acad Sci U S A. 2002; 99:10958–10963. [PubMed: 12177417]

[3]. Norris AJ, Sartippour MR, Lu M, Park T, Rao JY, Jackson MI, Fukuto JM, Brooks MN. Nitroxyl inhibits breast tumor growth and angiogenesis. Int J Cancer. 2008; 122:1905–1910. [PubMed: 18076071]

[4]. Paolocci N, Jackson MI, Lopez BE, Miranda K, Tocchetti CG, Wink DA, Hobbs AJ, Fukuto JM. The pharmacology of nitroxyl (HNO) and its therapeutic potential: not just the Janus face of NO. Pharmacol Ther. 2007; 113:442–458. [PubMed: 17222913]

[5]. Paolocci N, Katori T, Champion HC, St John ME, Miranda KM, Fukuto JM, Wink DA, Kass DA. Positive inotropic and lusitropic effects of HNO/NO- in failing hearts: independence from beta-adrenergic signaling. Proc Natl Acad Sci U S A. 2003; 100:5537–5542. [PubMed: 12704230]

[6]. Pagliaro P, Mancardi D, Rastaldo R, Penna C, Gattullo D, Miranda KM, Feelisch M, Wink DA, Kass DA, Paolocci N. Nitroxyl affords thiol-sensitive myocardial protective effects akin to early preconditioning. Free Radic Biol Med. 2003; 34:33–43. [PubMed: 12498977]

[7]. Miranda KM, Paolocci N, Katori T, Thomas DD, Ford E, Bartberger MD, Espey MG, Kass DA, Feelisch M, Fukuto JM, Wink DA. A biochemical rationale for the discrete behavior of nitroxyl and nitric oxide in the cardiovascular system. Proc Natl Acad Sci U S A. 2003; 100:9196–9201. [PubMed: 12865500]

[8]. Wink DA, Miranda KM, Katori T, Mancardi D, Thomas DD, Ridnour L, Espey MG, Feelisch M, Colton CA, Fukuto JM, Pagliaro P, Kass DA, Paolocci N. Orthogonal properties of the redox siblings nitroxyl and nitric oxide in the cardiovascular system: a novel redox paradigm. Am J Physiol Heart Circ Physiol. 2003; 285:H2264–2276. [PubMed: 12855429]

[9]. Fukuto JM, Jackson MI, Kaludercic N, Paolocci N. Examining nitroxyl in biological systems. Methods Enzymol. 2008; 440:411–431. [PubMed: 18423233]

[10]. Irvine JC, Ritchie RH, Favaloro JL, Andrews KL, Widdop RE, Kemp-Harper BK. Nitroxyl (HNO): the Cinderella of the nitric oxide story. Trends Pharmacol Sci. 2008; 29:601–608. [PubMed: 18835046]

[11]. Miranda KM. The chemistry of nitroxyl (HNO) and implications in biology. Coordination Chemistry Reviews. 2005; 249:433.

[12]. Ishimura Y, Gao YT, Panda SP, Roman LJ, Masters BS, Weintraub ST. Detection of nitrous oxide in the neuronal nitric oxide synthase reaction by gas chromatography-mass spectrometry. Biochem Biophys Res Commun. 2005; 338:543–549. [PubMed: 16154533]

[13]. Cho JY, Dutton A, Miller T, Houk KN, Fukuto JM. Oxidation of N-hydroxyguanidines by copper(II): model systems for elucidating the physiological chemistry of the nitric oxide biosynthetic intermediate N-hydroxyl-L-arginine. Arch Biochem Biophys. 2003; 417:65–76. [PubMed: 12921781]

[14]. Fukuto JM, Dutton AS, Houk KN. The chemistry and biology of nitroxyl (HNO): a chemically unique species with novel and important biological activity. Chembiochem. 2005; 6:612–619. [PubMed: 15619720]

[15]. Doyle MP, Mahapatro SN, Broene RD, Guy JK. Oxidation and reduction of hemoproteins by trioxodinitrate(II). The role of nitrosyl hydride and nitrite. Journal of the American Chemical Society. 1988; 110:593.

[16]. Marti MA, Bari SE, Estrin DA, Doctorovich F. Discrimination of Nitroxyl and Nitric Oxide by Water-Soluble Mn(III) Porphyrins. Journal of the American Chemical Society. 2005; 127:4680. [PubMed: 15796534]

[17]. Xia Y, Cardounel AJ, Vanin AF, Zweier JL. Electron paramagnetic resonance spectroscopy with N-methyl-D-glucamine dithiocarbamate iron complexes distinguishes nitric oxide and nitroxyl anion in a redox-dependent manner: applications in identifying nitrogen monoxide products from nitric oxide synthase. Free Radic Biol Med. 2000; 29:793–797. [PubMed: 11053782]

[18]. Donzelli S, Espey MG, Thomas DD, Mancardi D, Tocchetti CG, Ridnour LA, Paolocci N, King SB, Miranda KM, Lazzarino G, Fukuto JM, Wink DA. Discriminating formation of HNO from other reactive nitrogen oxide species. Free Radic Biol Med. 2006; 40:1056–1066. [PubMed: 16540401]

[19]. Cline MR, Tu C, Silverman DN, Toscano JP. Detection of nitroxyl (HNO) by membrane inlet mass spectrometry. Free Radical Biology and Medicine. 2011; 50:1274–1279. [PubMed: 21349325]

[20]. Rosenthal J, Lippard SJ. Direct Detection of Nitroxyl in Aqueous Solution Using a Tripodal Copper(II) BODIPY Complex. Journal of the American Chemical Society. 2010; 132:5536. [PubMed: 20355724]

[21]. Reisz JA, Zink CN, King SB. Rapid and selective nitroxyl (HNO) trapping by phosphines: kinetics and new aqueous ligations for HNO detection and quantitation. Journal of the American Chemical Society. 2011; 133:11675–11685. [PubMed: 21699183]

[22]. Akaike T, Yoshida M, Miyamoto Y, Sato K, Kohno M, Sasamoto K, Miyazaki K, Ueda S, Maeda H. Antagonistic action of imidazolineoxyl N-oxides against endothelium-derived relaxing factor/.NO through a radical reaction. Biochemistry. 1993; 32:827–832. [PubMed: 8422387]

[23]. Yoshida M, Akaike T, Wada Y, Sato K, Ikeda K, Ueda S, Maeda H. Therapeutic effects of imidazolineoxyl N-oxide against endotoxin shock through its direct nitric oxide-scavenging activity. Biochem Biophys Res Commun. 1994; 202:923–930. [PubMed: 8048966]

[24]. Mitaka C, Hirata Y, Yokoyama K, Nagura T, Tsunoda Y, Amaha K. Beneficial effect of carboxy-PTIO on hemodynamic and blood gas changes in septic shock dogs. Crit Care. 1997; 1:45–50. [PubMed: 11056696]

[25]. Konorev EA, Tarpey MM, Joseph J, Baker JE, Kalyanaraman B. S-nitrosoglutathione improves functional recovery in the isolated rat heart after cardioplegic ischemic arrest-evidence for a cardioprotective effect of nitric oxide. J Pharmacol Exp Ther. 1995; 274:200–206. [PubMed: 7616400]

[26]. Cabrales P, Tsai AG, Intaglietta M. Nitric oxide regulation of microvascular oxygen exchange during hypoxia and hyperoxia. J Appl Physiol. 2006; 100:1181–1187. [PubMed: 16357070]

[27]. Pieper GM, Siebeneich W. Use of a nitronyl nitroxide to discriminate the contribution of nitric oxide radical in endothelium-dependent relaxation of control and diabetic blood vessels. J Pharmacol Exp Ther. 1997; 283:138–147. [PubMed: 9336318]

[28]. Joseph J, Kalyanaraman B, Hyde JS. Trapping of nitric oxide by nitronyl nitroxides: an electron spin resonance investigation. Biochem Biophys Res Commun. 1993; 192:926–934. [PubMed: 8387295]

[29]. Woldman Y, Khramtsov VV, Grigor'ev IA, Kiriljuk IA, Utepbergenov DI. Spin trapping of nitric oxide by nitronylnitroxides: measurement of the activity of no synthase from rat cerebellum. Biochem Biophys Res Commun. 1994; 202:195–203. [PubMed: 7518673]

[30]. Akaike T, Maeda H. Quantitation of nitric oxide using 2-phenyl-4,4,5,5-tetramethylimidazoline-1-oxyl 3-oxide (PTIO). Methods Enzymol. 1996; 268:211–221. [PubMed: 8782587]

[31]. Azma T, Fujii K, Yuge O. Reaction between imidazolineoxil N-oxide (carboxy-PTIO) and nitric oxide released from cultured endothelial cells: quantitative measurement of nitric oxide by ESR spectrometry. Life Sci. 1994; 54:PL185–190. [PubMed: 8107514]

[32]. Bobko AA, Bagryanskaya EG, Reznikov VA, Kolosova NG, Clanton TL, Khramtsov VV. Redox-sensitive mechanism of no scavenging by nitronyl nitroxides. Free Radic Biol Med. 2004; 36:248–258. [PubMed: 14744636]

[33]. Goldstein S, Russo A, Samuni A. Reactions of PTIO and carboxy-PTIO with *NO, *NO2, and O2-*. J Biol Chem. 2003; 278:50949–50955. [PubMed: 12954619]

[34]. Hogg N, Singh RJ, Joseph J, Neese F, Kalyanaraman B. Reactions of nitric oxide with nitronyl nitroxides and oxygen: prediction of nitrite and nitrate formation by kinetic simulation. Free Radic Res. 1995; 22:47–56. [PubMed: 7889147]

[35]. Samuni U, Samuni Y, Goldstein S. On the Distinction between Nitroxyl and Nitric Oxide Using Nitronyl Nitroxides. Journal of the American Chemical Society. 2010; 132:8428. [PubMed: 20504018]

[36]. Hrabie JA, Klose JR, Wink DA, Keefer LK. New nitric oxide-releasing zwitterions derived from polyamines. The Journal of Organic Chemistry. 1993; 58:1472.

[37]. Chao S, Simon RA, Mallouk TE, Wrighton MS. Multicomponent redox catalysts for reduction of large biological molecules using molecular hydrogen as the reductant. Journal of the American Chemical Society. 1988; 110:2270.

[38]. MacDonald RC, MacDonald RI, Menco BPM, Takeshita K, Subbarao NK, Hu L.- r. Small-volume extrusion apparatus for preparation of large, unilamellar vesicles. Biochimica et Biophysica Acta (BBA) - Biomembranes. 1991; 1061:297.

[39]. Hughes MN, Wimbledon PE. The chemisry of trioxodinitrates. Part I. Decompostion of sodium trioxodinitrate (Angeli's salt) in aqueous solution. Journal Chemical Society, Dalton Transaction. 1976:703–707.

[40]. Bonner FT, Dzelzkalns LS, Bonucci JA. Properties of nitroxyl as intermediate in the nitric oxide-hydroxylamine reaction and in trioxodinitrate decomposition. Inorganic Chemistry. 1978; 17:2487.

[41]. Goldstein S, Samuni A, Russo A. Reaction of Cyclic Nitroxides with Nitrogen Dioxide: The Intermediacy of the Oxoammonium Cations. Journal of the American Chemical Society. 2003; 125:8364. [PubMed: 12837108]

[42]. Singh RJ, Hogg N, Joseph J, Konorev E, Kalyanaraman B. The Peroxynitrite Generator, SIN-1, Becomes a Nitric Oxide Donor in the Presence of Electron Acceptors. Archives of Biochemistry and Biophysics. 1999; 361:331. [PubMed: 9882464]

[43]. Murphy ME, Sies H. Reversible conversion of nitroxyl anion to nitric oxide by superoxide dismutase. Proc Natl Acad Sci U S A. 1991; 88:10860–10864. [PubMed: 1961756]

[44]. Jackson MI, Han TH, Serbulea L, Dutton A, Ford E, Miranda KM, Houk KN, Wink DA, Fukuto JM. Kinetic feasibility of nitroxyl reduction by physiological reductants and biological implications. Free Radical Biology and Medicine. 2009; 47:1130. [PubMed: 19577638]

[45]. Haseloff RF, Zollner S, Kirilyuk IA, Grigor'ev IA, Reszka R, Bernhardt R, Mertsch K, Roloff B, Blasig IE. Superoxide-mediated reduction of the nitroxide group can prevent detection of nitric oxide by nitronyl nitroxides. Free Radic Res. 1997; 26:7–17. [PubMed: 9018468]

[46]. Woldman YY, Semenov SV, Bobko AA, Kirilyuk IA, Polienko JF, Voinov MA, Bagryanskaya EG, Khramtsov VV. Design of liposome-based pH sensitive nanoSPIN probes: nano-sized particles with incorporated nitroxides. Analyst. 2009; 134:904–910. [PubMed: 19381383]

[47]. Yelinova VI, Bobko AA, Mazhukin DG, Markel AL, Khramtsov VV. New Donors and Acceptors of Nitrogen Oxide as Potential Therapeutic Agents. Russian Journal of Bioorganic Chemistry. 2003; 29:395.

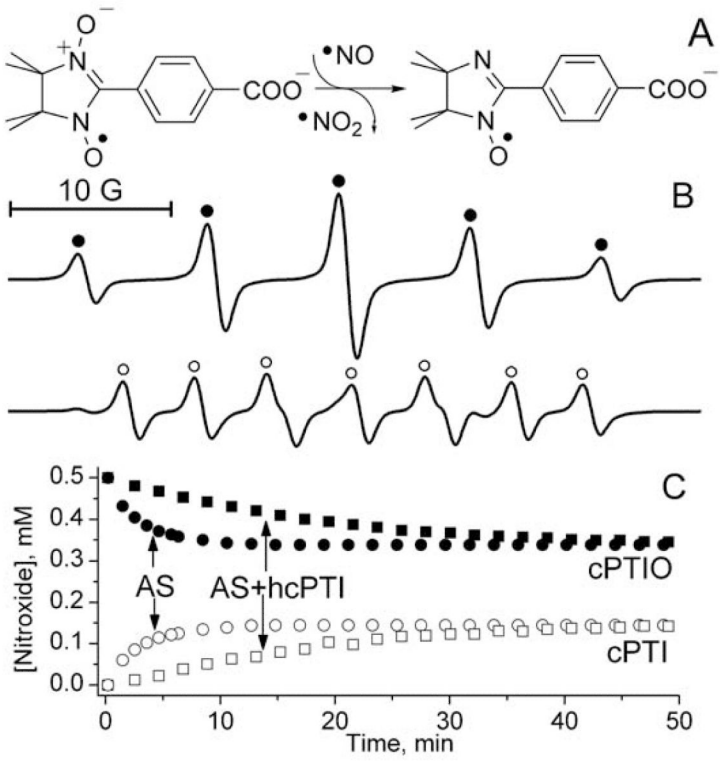

Figure 1.

A. Scheme of the reaction of cPTIO with •NO producing cPTI and •NO_2. **B.** The EPR spectra of 0.5 mM solutions of cPTIO (•; $a_{N1}=a_{N3}=8.1$ G) and cPTI (o; $a_{N1}=9.8$ G, $a_{N3}=4.6$ G). The solution of cPTI was obtained upon titration of cPTIO solution with •NO donor, Proli NONOate, as described in Materials and Methods. **C**. The reaction of cPTIO with Angeli's salt: the kinetics of cPTIO decay (filled symbols) and cPTI formation (empty symbols) were measured by EPR in solution of 0.5 mM cPTIO after addition of 0.16 mM AS alone (o) or 0.16 mM AS and 0.5 mM hydroxylamine, hcPTI (□).

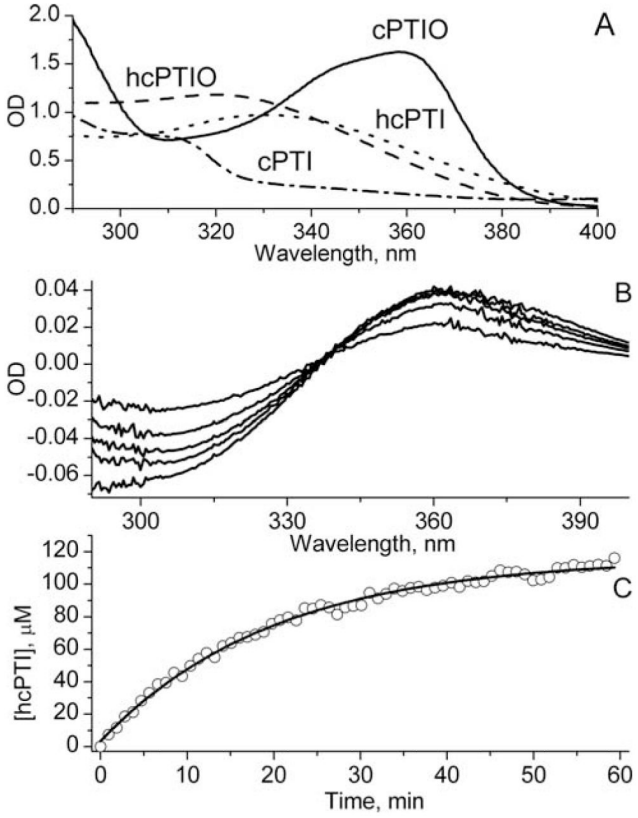

Figure 2.

A. The optical spectra of 0.6 mM solutions of cPTIO (—), hcPTIO (---), cPTI (-·-·-) and hcPTI (·····). Spectra were recorded in quartz cuvette with light pass 4 mm. hcPTIO and hcPTI were prepared by reduction with 0.25 mM ascorbic acid. **B**. Representative differential optical spectra of mixture of 0.4 mM cPTIO and 0.2 mM hcPTIO after addition of 125 μM Angeli's salt measured at time points 6.6, 13.2, 19.8, 26.4 and 46.1 min. Spectra were recorded in cuvette with light pass 4 mm. **C.** The kinetics of hcPTI formation from hcPTIO calculated using differential extinction coefficient at wavelength 299 nm, ε_{299} (hcPTIO/hcPTI) = 1.5 $mM^{-1}cm^{-1}$. Solid line represents the monoexponential approximation with $\tau_{1/2}$=(14±1) min.

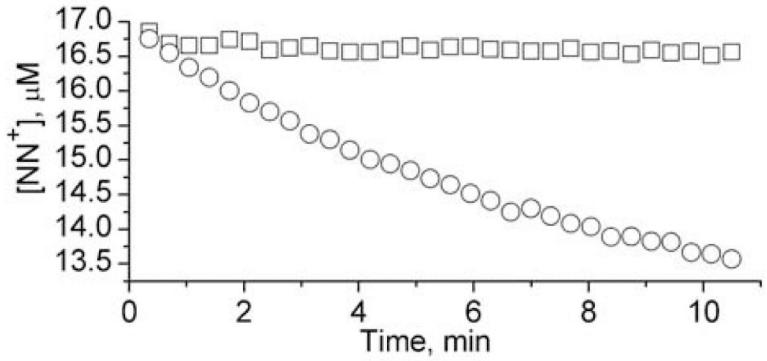

Figure 3.

Kinetics of the decay of liposome-encapsulated NN^+ measured by EPR during enzymatic generation of HNO (○). HNO was generated by catalase, 2 mg/ml, from cyanamide, 10 mM, in the presence of 5 U/ml glucose oxidase and 5 mM glucose[43]. Addition of glucose oxidase/glucose was used as a source of hydrogen peroxide. The symbols (□) denote the kinetics measured in the same system but in the presence of 1 mM glutathione.

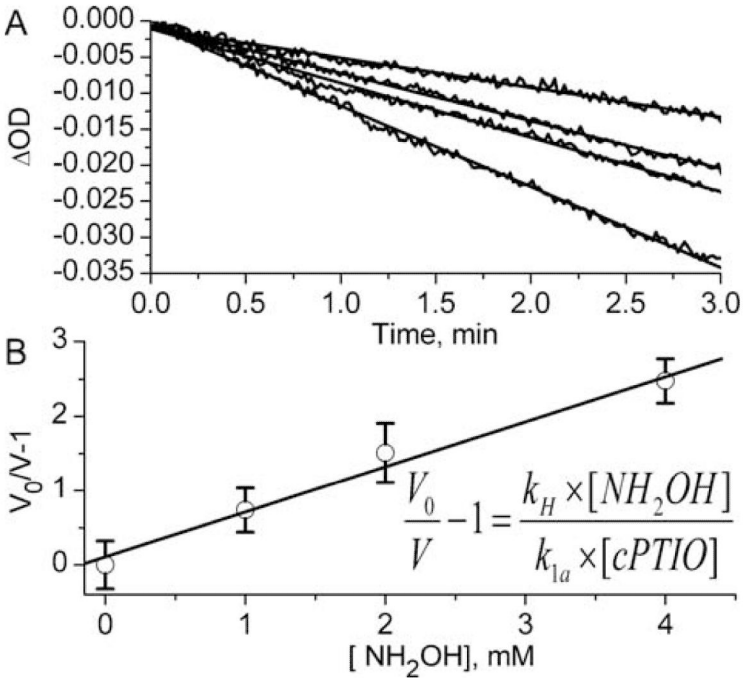

Figure 4.

The measurement of the rate constant of the reaction of cPTIO with HNO using NH_2OH as competitive agent. (**A**) The decrease of absorbance at 299 nm in the mixture of 0.3 mM cPTIO and 0.3 mM hcPTIO measured after addition of 0.5 mM Angeli's salt in the presence of various concentrations of NH_2OH. Lines represent linear fits yielding the rates of hcPTI formation to be equal to 31, 21, 18, and 11 μM/s for 0, 1, 2, and 4 mM NH_2OH, correspondingly (from bottom upwards). (**B**) The dependence of (V_0/V-*1*) term on NH_2OH concentration calculated from Figure 4A. Line represents linear fit yielding k_{1a} = (5.5±0.9) ×k_H.

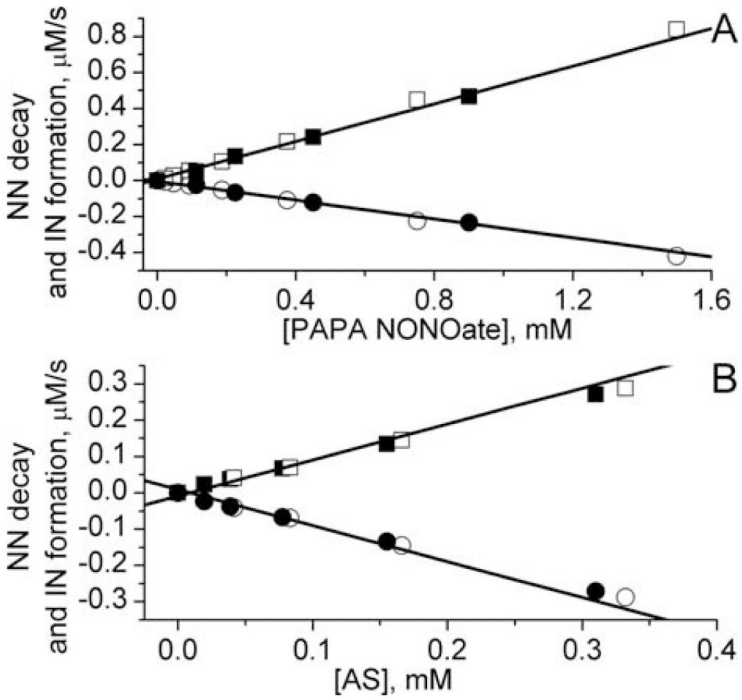

Figure 5.

The dependencies of the rates of NN decay (○) and IN formation (□) on concentration of PAPA NONOate (**A**) and AS (**B**) measured by EPR using 0.5 mM cPTIO/0.5 mM hcPTI (filled symbols) or 0.5 mM NN^+/5 mM hIN^+ (empty symbols). Lines represent linear approximations yielding half lifetime of PAPA NONOate and AS decomposition $\tau_{1/2}$ = (88±2) min and $\tau_{1/2}$ = (14.0±0.2) min, correspondingly. The stoichiometry values Δ[IN]/Δ[NN] were found to be equal to 1.9±0.1 (**A**) and 0.95±0.07 (**B**).

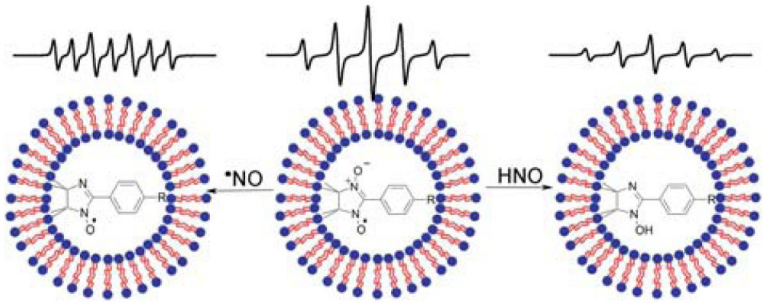

Figure 6.

Schematic design of liposome-encapsulated paramagnetic sensor for the discriminative EPR detection of •NO and HNO. Encapsulation protects NN^+ ($R=N^+(CH_3)_3$) from reducing agents. Both •NO and HNO freely diffuse across the phospholipid membrane, then react with the NN^+ resulting in formation of different products, paramagnetic IN^+ and diamagnetic hydroxylamine hIN^+, correspondingly. The EPR spectra illustrate corresponding transformation of quintet spectral pattern of NN^+ to septet spectral pattern of IN^+, or decay of the EPR signal upon formation of EPR-silent hIN^+.

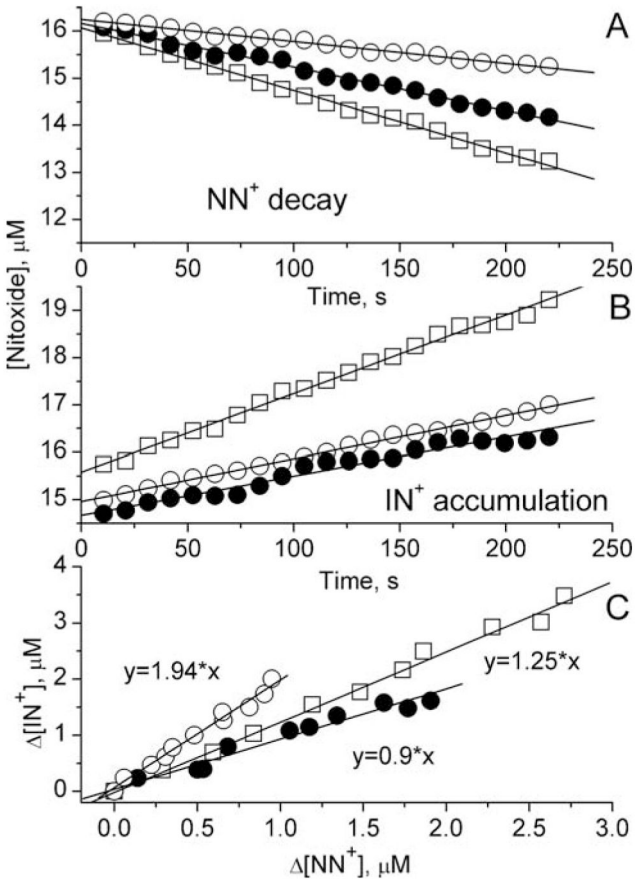

Figure 7.

EPR monitoring of •NO and/or HNO release by liposome-encapsulated detection system (0.5 mM NN^+, 0.5 mM IN^+ and 5 mM hIN^+). The kinetics of NN^+ decay (**A**) and IN^+ accumulation (**B**) were measured after initiation of •NO or/and HNO generation by addition of 18 μM PAPA NONOate (○), 11 μM AS (•), or PAPA NONOate and AS together (□). Solid lines in panels **A** and **B** represent linear fits yielding the rates of NN^+ decay and IN^+ accumulation presented in the Table 1. Panel **C** shows the dependences of $\Delta[IN^+]$ on $\Delta[NN^+]$ calculated from the data in panels A and B.

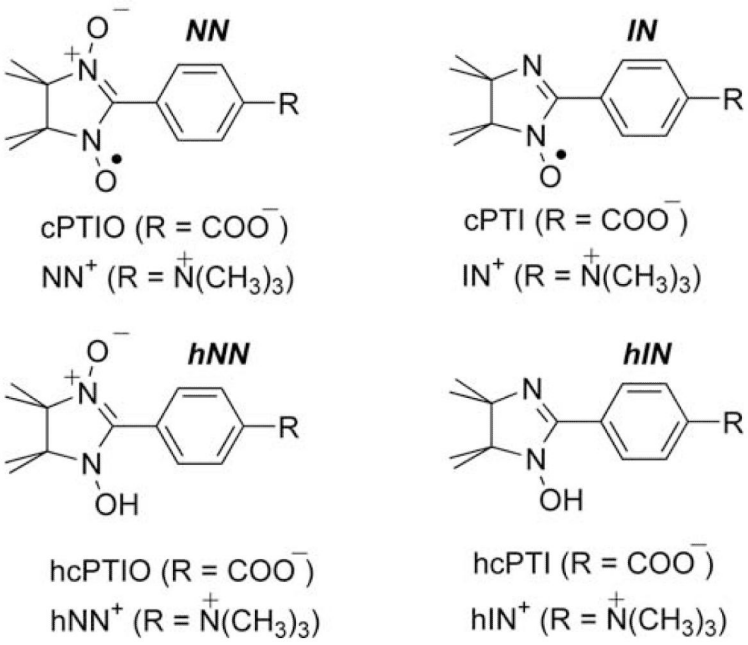

Scheme 1.

Chemical structures of the NNs (cPTIO and NN^+), INs (cPTI and IN^+) and corresponding hydroxylamines, hNNs (hcPTIO and hNN^+) and hINs (hcPTI and hIN^+) discussed in this work.

Table 1

The rates of the NN^+ decay, IN^+ increase and stoichiometry $\Delta[IN]/\Delta[NN]$ measured by EPR using liposome-encapsulated detection system upon generation of $^{\bullet}NO$, HNO and both species (see Fig. 7).

	$^{\bullet}NO$	HNO	$^{\bullet}no+hno$
Rate[a], nM/s	4.7	9.2	13.9
$-d[NN^+]/dt$, nM/s	4.7±0.5	9.2±0.5	13.3±0.5
$d[IN^+]/dt$, nM/s	9.1±0.5	8.3±0.5	16.7±0.5
$\Delta[IN^+]/\Delta[NN^+]$ (calculated)	1.9±0.2 (2)	0.9±0.1 (1)	1.25±0.05 (1.34[b])

[a] The rates of $^{\bullet}NO$ or HNO generations were calculated using half lifetimes of PAPA NONOate and AS decompositions obtained in the same experimental conditions as shown in Fig. 5.

[b] For the simultaneous $^{\bullet}NO$ and HNO generation the stoichiometry $\Delta[IN^+]/\Delta[NN^+]$ was calculated using the rates of generation of these species[a] and assuming the values $\Delta[IN^+]/\Delta[NN^+]$ for NN^+ reaction with $^{\bullet}NO$ and HNO being equal to 2 and 1, correspondingly.